

Anomaly Detection Under Multiplicative Noise Model Uncertainty

Venkatraman Renganathan*, Benjamin J. Gravell*, Justin Ruths, and Tyler H. Summers

Abstract—State estimators are crucial components of anomaly detectors that are used to monitor cyber-physical systems. Many frequently-used state estimators are susceptible to model risk as they rely critically on the availability of an accurate state-space model. Modeling errors make it more difficult to distinguish whether deviations from expected behavior are due to anomalies or simply a lack of knowledge about the system dynamics. In this research, we account for model uncertainty through a multiplicative noise framework. Specifically, we propose to use the multiplicative noise LQG based compensator in this setting to hedge against the model uncertainty risk. The size of the residual from the estimator can then be compared against a threshold to detect anomalies. Finally, the proposed detector is validated using numerical simulations. Extension of state-of-the-art anomaly detection in cyber-physical systems to handle model uncertainty represents the main novel contribution of the present work.

I. INTRODUCTION

Cyber-Physical Systems (CPS) are physical processes that are tightly integrated with computation and communication systems for monitoring and control. Though advances in CPS design has equipped them with adaptability, resiliency, safety, and security features that exceed the simple embedded systems of the past, it often leaves open several points for attackers to strike. CPS security problems have attracted the attention of researchers worldwide recently; some state-of-the-art anomaly detection algorithms can be found in [1]–[3].

A common practice is to model a CPS as either a deterministic system or a stochastic system with additive Gaussian uncertainties. Motivated by the recent developments in distributionally robust optimization (DRO) techniques [4]–[6], authors in [7]–[9] have developed DRO anomaly detectors that remove assumptions on specific functional forms of the uncertainties in the stochastic CPS model. On the other hand, it is a common practice to assume that the true CPS dynamics are known exactly. Unfortunately, modeling and sampling errors are inherent and significant in working with real systems due to nonlinearities, learned (system identification, machine learning) models, adaptive models, or simply due to changing environmental conditions or aging. A multiplicative noise framework for capturing model uncertainty offers several compelling advantages over additive noise models. It provides a statistical description of the uncertainty that depends on the control input and state [10]–[12]. Using a multiplicative noise model, however, requires new tools to

build and tune anomaly detectors that accommodate the more general functional form of the model.

State estimation is a crucial component in any model-based anomaly detector design, which depends on a state-space model for the system dynamics. This dependency causes limitations on the usage of the classical Kalman filter as it critically relies on the availability of an accurate state-space model, making it susceptible to model risk. Robust Kalman filtering with additive uncertainties was explored in [13], where the uncertain joint distribution of the states and outputs was accounted for. Another robust Kalman filter design was developed using a τ -divergence based family of distributions in [14]. In [15], a Wasserstein distributionally robust Kalman filter (W-DR-KF) was developed to account for distributional uncertainty. However, a procedure for jointly computing a pair of state estimator and feedback gain to guarantee stability in this setting remains unexplored.

Although stochastic modeling of CPS with additive uncertainty is well studied, there are no works to the best of our knowledge which have considered both multiplicative and additive noises together in the CPS security literature. The evolution of non-Gaussian state distributions under the effect of multiplicative noise invalidates use of the standard Kalman filter, as the separation principle available in linear quadratic Gaussian (LQG) setting in [16] no longer holds. Though [10] considered both multiplicative and additive noises in an optimal control setting, a restrictive Gaussian assumption was imposed on the uncertainties. The approach in this paper builds on the foundation established by [17], where the multiplicative noise-driven LQG (MLQG) problem was solved by posing a set of coupled algebraic Riccati equations, from which the optimal linear output feedback controller and estimator gains were jointly computed.

Contributions: This paper is part of our ongoing work [7], [8] to leverage powerful results in control theory and distributionally robust optimization to design robust anomaly detectors. Specifically, the detector threshold corresponding to a desired false alarm rate in the setting considered in this paper was computed through the moment-based approaches explained [7]. In prior work we addressed detectors robust to non-Gaussian additive noise. In this work,

- 1) We design an anomaly detector for stochastic linear cyber-physical systems that is robust to modeling errors. To our knowledge, this is the first paper to consider tuning an anomaly detector for a system model that incorporates model uncertainty. We propose a multiplicative noise framework and integrate the MLQG compensator to compute the residual.
- 2) We demonstrate our proposed approach using numer-

*Equal contribution of these authors. V. Renganathan is with the Department of Automatic Control, Lund University, Sweden. B.J. Gravell, J. Ruths, and T.H. Summers are with the Department of Mechanical Engineering at The University of Texas at Dallas, Richardson, TX, USA. E-mail: venkat@control.lth.se, [\(benjamin.gravell,jruths,tyler.summers\)@utdallas.edu](mailto:(benjamin.gravell,jruths,tyler.summers)@utdallas.edu).

ical simulations and show that multiplicative noises result in greater anomaly detector thresholds as long as mean square compensatability conditions are satisfied.

The rest of the paper is organized as follows. In §II, the problem of monitoring an uncertain CPS with model uncertainty is formulated. Then, the multiplicative noise driven LQG compensator is discussed in §III. Subsequently, the anomaly detector design is presented in §IV. The proposed idea is then demonstrated using a numerical simulation in §V. Finally, the paper is closed in §VI along with directions for future research.

NOTATIONS & PRELIMINARIES

The set of real numbers, integers are denoted by \mathbb{R}, \mathbb{Z} . The subset of real numbers greater than $a \in \mathbb{R}$ is denoted by $\mathbb{R}_{>a}$. The set of integers between two values $a, b \in \mathbb{Z}$ with $a < b$ is denoted by $[a : b]$. We denote by \mathbb{S}^n the set of symmetric matrices in $\mathbb{R}^{n \times n}$ and the cone of positive definite (semi-definite) matrices on \mathbb{S}^n as $\mathbb{S}_{++}^n(\mathbb{S}_+^n)$. An identity matrix in dimension n is denoted by I_n . The Kronecker product of two matrices $A \in \mathbb{R}^{m \times n}, B \in \mathbb{R}^{p \times q}$ is denoted by $A \otimes B$ and the vectorization of a matrix $A \in \mathbb{R}^{m \times n}$ is denoted by $\text{vec}(A) \in \mathbb{R}^{mn}$ and the matricization of vector $x \in \mathbb{R}^p$ is denoted by $\text{mat}(x, n, m) \in \mathbb{R}^{n \times m}$ where $n \times m = p$. The trace of a matrix $A \in \mathbb{R}^{n \times n}$ is denoted by $\text{Tr}(A)$. A probability distribution with mean μ and covariance Σ is denoted by $\mathbb{P}(\mu, \Sigma)$, and specifically $\mathcal{N}_d(\mu, \Sigma)$ if the distribution is normal in \mathbb{R}^d . Given a matrix $A \in \mathbb{R}^{n \times n}$ and a vector valued random variable $z \in \mathbb{R}^p, p \geq 1$ with $\mathbb{E}[z] = \mu, \mathbb{E}[(z - \mu)(z - \mu)^\top] = \Sigma$, then $\mathbb{E}[z^\top Az] = \text{Tr}(A\Sigma) + \mu^\top A\mu$.

II. PROBLEM FORMULATION

A. Uncertain CPS Model

We model an uncertain CPS for time $k \in \mathbb{N}$ using a stochastic discrete-time linear time varying (LTV) system:

$$x_{k+1} = A_k x_k + B_k u_k + w_k, \quad (1)$$

$$y_k = C_k x_k + v_k. \quad (2)$$

Here, $x_k \in \mathbb{R}^n$, $u_k \in \mathbb{R}^m$, and $y_k \in \mathbb{R}^p$ are the system state, control input, and output at time k . The next-state $x_{k+1} \in \mathbb{R}^n$ is a random linear combination of the current state and process noise w_k , which is a zero-mean white noise process. Similarly, the output $y_k \in \mathbb{R}^p$ is a random linear combination of the states and the sensor noise v_k , which is a zero-mean white noise process. The initial state is a random variable $x_0 \sim \mathbb{P}_{x_0}(0, \Sigma_{x_0})$. The system matrices are decomposed as

$$A_k = (\bar{A} + \hat{A}_k), \quad B_k = (\bar{B} + \hat{B}_k), \quad C_k = (\bar{C} + \hat{C}_k),$$

$$\hat{A}_k = \sum_{i=1}^{n_a} \gamma_{ki} \mathcal{A}_i, \quad \hat{B}_k = \sum_{j=1}^{n_b} \delta_{kj} \mathcal{B}_j, \quad \hat{C}_k = \sum_{l=1}^{n_c} \kappa_{kl} \mathcal{C}_l. \quad (3)$$

where $\bar{A}, \bar{B}, \bar{C}$ denote the nominal dynamics, control, and output matrices respectively. The multiplicative noise terms are modeled by the i.i.d. across time (white), zero-mean, mutually independent scalar random variables $\gamma_{ki}, \delta_{kj}, \kappa_{kl}$,

which have variances $\sigma_{a,i}^2, \sigma_{b,j}^2, \sigma_{c,l}^2$ for $i \in [1 : n_a], j \in [1 : n_b], l \in [1 : n_c]$ respectively with $n_a, n_b, n_c \in \mathbb{Z}_{>0}$. The pattern matrices $\mathcal{A}_i \in \mathbb{R}^{n \times n}, \mathcal{B}_j \in \mathbb{R}^{n \times m}$, and $\mathcal{C}_l \in \mathbb{R}^{p \times n}$ specify how each scalar noise term affects the system matrices. It is then evident from (1) and (2) that \hat{A}_k, \hat{B}_k , and \hat{C}_k quantify uncertainty about the nominal system matrices A, B , and C respectively. The distributions of all the scalar multiplicative noise random variables are assumed to be known. On the other hand, the distributions of the process noise \mathbb{P}_w and measurement noise \mathbb{P}_v are not known exactly¹, but reside in the moment-based ambiguity sets

$$\mathcal{P}^w := \{ \mathbb{P}_w \mid \mathbb{E}[w_k] = 0, \mathbb{E}[w_k w_k^\top] = \Sigma_w \}, \quad (4)$$

$$\mathcal{P}^v := \{ \mathbb{P}_v \mid \mathbb{E}[v_k] = 0, \mathbb{E}[v_k v_k^\top] = \Sigma_v \}, \quad (5)$$

where the covariance (Σ_w, Σ_v) are assumed known; they may be estimated from collected data via e.g. bootstrap sample averaging. For simplicity, we assume that x_0 and all the additive, multiplicative noises $w_k, v_k, \{\gamma_{ki}\}_{i=1}^{n_a}, \{\delta_{kj}\}_{j=1}^{n_b}, \{\kappa_{kl}\}_{l=1}^{n_c}$ are mutually independent of each other. We denote the first moment, second moment, and covariance of the state at time k as $\mu_{x_k} = \mathbb{E}[x_k]$, $V_k = \mathbb{E}[x_k x_k^\top]$, and $\Sigma_{x_k} = \mathbb{E}[(x_k - \mu_{x_k})(x_k - \mu_{x_k})^\top]$, respectively. Likewise, we denote the first moment, second moment, and covariance of the output at time k as $\mu_{y_k} = \mathbb{E}[y_k]$, $Y_k = \mathbb{E}[y_k y_k^\top]$, and $\Sigma_{y_k} = \mathbb{E}[(y_k - \mu_{y_k})(y_k - \mu_{y_k})^\top]$, respectively.

B. Review of Concepts

Here, we re-state some definitions from [17] on the mean squared versions of stabilizability, detectability and the resulting compensatability of systems given by (1) and (2).

Definition 1: The system in (1) is *mean-square stable* if $\forall x_0 \in \mathbb{R}^n, \exists V_\infty \in \mathbb{S}_+^n$ such that

$$\lim_{k \rightarrow \infty} V_k = \lim_{k \rightarrow \infty} \mathbb{E}[x_k x_k^\top] \rightarrow V_\infty.$$

Definition 2: The system in (1) is *mean-square stabilizable* if there exists a control gain matrix $K \in \mathbb{R}^{m \times n}$ such that using controls $u_k = K x_k$ makes (1) mean-square stable.

Definition 3: The system in (1) and (2) is *mean-square compensatable* if there exist control and filter gain matrices $K \in \mathbb{R}^{m \times n}$ and $L \in \mathbb{R}^{n \times p}$ such that the system

$$\begin{bmatrix} x_{k+1} \\ \hat{x}_{k+1} \end{bmatrix} = \begin{bmatrix} A_k & B_k K \\ L C_k & \bar{A} + \bar{B} K - L \bar{C} \end{bmatrix} \begin{bmatrix} x_k \\ \hat{x}_k \end{bmatrix}$$

is mean-square stable.

Assumptions

- 1) The system given by (1) and (2) is *mean-square compensatable*.
- 2) The optimal state estimator at any time k given (1) and (2) is an affine² function of the output y_k .

Problem 1: Under the above assumptions for a given stochastic CPS model specified by (1), (2), obtain residual

¹Even when $\mathbb{P}_w, \mathbb{P}_v, \mathbb{P}_{x_0}$ are assumed to be Gaussian, \mathbb{P}_{x_k} at any time step $k > 0$ due to (1) will be *non-Gaussian* due to the multiplicative noise.

²It is possible to design a nonlinear state estimator to outperform a given affine estimator in this setting. However, it is out of the scope of this paper.

data from an appropriate state estimator module that accounts for both multiplicative and additive noises, and subsequently design an anomaly detector threshold such that the worst case false alarm rate does not exceed a desired value.

III. RESIDUALS VIA MULTIPLICATIVE NOISE LQG

Due to the multiplicative noises in (1) and (2), the state distribution will be non-Gaussian even when all primitive noise distributions are Gaussian. Further, the classical separation principle from the additive noise setting does not hold in presence of multiplicative noises [17]. This necessitates a framework where the optimal controller and the estimator gains are computed *jointly*. Here, we elaborate on obtaining the residual from CPS using the multiplicative noise-driven LQG and show that the residual covariance is a function of both additive and multiplicative noise covariance matrices.

A. Designing Multiplicative Noise-Driven LQG

Under both multiplicative and additive noises in the system, the optimal linear output feedback controller can be exactly computed through the combination of a multiplicative noise KF with a multiplicative noise LQR as described in [10], [17], [18]. We consider the multiplicative noise-driven linear-quadratic Gaussian (MLQG) optimal control problem, which requires finding an output feedback controller $u_k = \pi_k(y_{0:k})$ for a system given by (1) and (2):

$$\underset{\pi_k \in \Pi_k}{\text{minimize}} \quad \lim_{T \rightarrow \infty} \frac{1}{T} \mathbb{E}_{\mathcal{E}_k} \left[\sum_{k=0}^{T-1} x_k^\top Q x_k + u_k^\top R u_k \right], \quad (6)$$

subject to (1), (2),

where $\mathcal{E}_k = \left\{ x_0, \{\hat{A}_k\}, \{\hat{B}_k\}, \{\hat{C}_k\}, \{w_k\}, \{v_k\} \right\}$, $Q \succeq 0$, $R \succ 0$. Then, the optimal linear compensator gain matrices can be computed by solving the following coupled nonlinear matrix Riccati equations in symmetric matrix variables $P_1, P_2, P_3, P_4 \in \mathbb{S}_+^n$:

$$\begin{aligned} P_1 &= Q + \bar{A}^\top P_1 \bar{A} + \sum_{i=1}^{n_a} \sigma_{a,i}^2 \mathcal{A}_i^\top P_1 \mathcal{A}_i - K^\top K_\alpha K \\ &\quad + \sum_{i=1}^{n_a} \sigma_{a,i}^2 \mathcal{A}_i^\top P_2 \mathcal{A}_i + \sum_{i=1}^{n_c} \sigma_{c,i}^2 \mathcal{C}_i^\top L^\top P_2 L \mathcal{C}_i, \end{aligned} \quad (7)$$

$$P_2 = (\bar{A} - L \bar{C})^\top P_2 (\bar{A} - L \bar{C}) + K^\top K_\alpha K, \quad (8)$$

$$\begin{aligned} P_3 &= \Sigma_w + \bar{A} P_3 \bar{A}^\top - L L_\alpha L^\top + \sum_{i=1}^{n_a} \sigma_{a,i}^2 \mathcal{A}_i P_3 \mathcal{A}_i^\top \\ &\quad + \sum_{i=1}^{n_a} \sigma_{a,i}^2 \mathcal{A}_i P_4 \mathcal{A}_i^\top + \sum_{i=1}^{n_b} \sigma_{b,i}^2 \mathcal{B}_i K P_4 K^\top \mathcal{B}_i^\top, \end{aligned} \quad (9)$$

$$P_4 = (\bar{A} + \bar{B} K) P_4 (\bar{A} + \bar{B} K)^\top + L L_\alpha L^\top, \quad (10)$$

where for notation simplicity, we denote

$$K_\alpha = R + \bar{B}^\top P_1 \bar{B} + \sum_{j=1}^{n_b} \sigma_{b,j}^2 \mathcal{B}_j^\top P_1 \mathcal{B}_j + \sum_{j=1}^{n_b} \sigma_{b,j}^2 \mathcal{B}_j^\top P_2 \mathcal{B}_j \quad (11)$$

$$L_\alpha = \Sigma_w + \bar{C} P_3 \bar{C}^\top + \sum_{j=1}^{n_c} \sigma_{c,j}^2 \mathcal{C}_j P_3 \mathcal{C}_j^\top + \sum_{j=1}^{n_c} \sigma_{c,j}^2 \mathcal{C}_j P_4 \mathcal{C}_j^\top. \quad (12)$$

Then, the associated optimal controller and estimator gains (K, L) are given by

$$K = -K_\alpha^{-1} \bar{B}^\top P_1 \bar{A}, \quad (13)$$

$$L = \bar{A} P_3 \bar{C}^\top L_\alpha^{-1}. \quad (14)$$

Finally, the optimal linear compensator is

$$u_k = K \hat{x}_k, \quad \text{and} \quad (15)$$

$$\begin{aligned} \hat{x}_{k+1} &= (\bar{A} + \bar{B} K) \hat{x}_k + L (y_k - \bar{C} \hat{x}_k), \\ &= (\bar{A} + \bar{B} K + L \hat{C}_k) \hat{x}_k + L C_k e_k + L v_k \end{aligned} \quad (16)$$

It is necessary to account for the multiplicative noise to achieve the minimum quadratic cost; furthermore, it is straightforward to find systems in (1) and (2) which are *mean-square unstable* when controlled by (multiplicative-noise-ignorant) LQG, meaning that it is necessary to account for multiplicative noise to achieve mean-square stability.

B. Residual from Multiplicative Noise LQG

We define the estimation error as $e_k = x_k - \hat{x}_k$. Then the estimation error evolves as follows

$$e_{k+1} = (\bar{A} - \hat{B}_k K - L C_k) e_k + (\hat{A}_k + \hat{B}_k K) x_k + w_k - L v_k. \quad (17)$$

We now elaborate how to obtain the residual signal required for anomaly detection. Define the residual $r_k \in \mathbb{R}^p$ as

$$r_k = y_k - \bar{C} \hat{x}_k = \bar{C} e_k + \hat{C}_k x_k + v_k \quad \text{and} \quad (18)$$

$$\mathbb{E}[r_k] = \mathbb{E}[y_k - \hat{y}_k] = \mathbb{E}[C_k x_k + v_k - \bar{C} \hat{x}_k] = \bar{C} e_k. \quad (19)$$

Then, r_k is not necessarily Gaussian due to the multiplicative noise and has mean $\mathbb{E}[r_k] = \bar{C} e_k$ (it becomes zero mean $\forall k \geq 0$ if $e_0 = 0$) with covariance matrix whose vectorized form is given by

$$R_k = (\bar{C} \otimes \bar{C}) E_k + \mathbb{E} \left[\hat{C}_k \otimes \hat{C}_k \right] X_k + \text{vec}(\Sigma_v). \quad (20)$$

To compute the steady state second moments of the residual r_k , we define

$$\begin{aligned} E_k &= \text{vec}(\mathbb{E}[e_k e_k^\top]), & X_k &= \text{vec}(\mathbb{E}[x_k x_k^\top]), \\ \tilde{X}_k &= \text{vec}(\mathbb{E}[x_k \hat{x}_k^\top]), & \tilde{X}_k &= \text{vec}(\mathbb{E}[\hat{x}_k x_k^\top]), \\ \hat{X}_k &= \text{vec}(\mathbb{E}[\hat{x}_k \hat{x}_k^\top]), & R_k &= \text{vec}(\mathbb{E}[r_k r_k^\top]) \end{aligned}$$

$$H = \begin{bmatrix} \bar{A} \otimes \bar{A} + \Sigma'_A & (\bar{B}K) \otimes \bar{A} & \bar{A} \otimes (\bar{B}K) & (\bar{B} \otimes \bar{B} + \Sigma'_B)(K \otimes K) \\ (\bar{L}\bar{C}) \otimes \bar{A} & (\bar{A} + \bar{B}K - L\bar{C}) \otimes \bar{A} & (\bar{L}\bar{C}) \otimes (\bar{B}K) & (\bar{A} + \bar{B}K - L\bar{C}) \otimes (\bar{B}K) \\ \bar{A} \otimes (L\bar{C}) & (\bar{B}K) \otimes (L\bar{C}) & \bar{A} \otimes (\bar{A} + \bar{B}K - L\bar{C}) & (\bar{B}K) \otimes (\bar{A} + \bar{B}K - L\bar{C}) \\ (L \otimes L)(\bar{C} \otimes \bar{C} + \Sigma'_C) & (\bar{A} + \bar{B}K - L\bar{C}) \otimes (L\bar{C}) & (\bar{L}\bar{C}) \otimes (\bar{A} + \bar{B}K - L\bar{C}) & (\bar{A} + \bar{B}K - L\bar{C}) \otimes (\bar{A} + \bar{B}K - L\bar{C}) \end{bmatrix}.$$

Fig. 1: The Matrix H in (21) with terms containing the second moments of entries of the vector \mathcal{X}_k .

$$\mathcal{X}_k := [X_k^\top \ \tilde{X}_k^\top \ \check{X}_k^\top \ \hat{X}_k^\top]^\top, \quad \mathcal{V} := \begin{bmatrix} \text{vec}(\Sigma_w) \\ \text{vec}(\Sigma_v) \end{bmatrix},$$

$$\Sigma'_A = \mathbb{E} [\hat{A}_k \otimes \hat{A}_k] = \sum_{i=1}^{n_a} \sigma_{a,i}^2 (\mathcal{A}_i \otimes \mathcal{A}_i),$$

$$\Sigma'_B = \mathbb{E} [\hat{B}_k \otimes \hat{B}_k] = \sum_{j=1}^{n_b} \sigma_{b,j}^2 (\mathcal{B}_j \otimes \mathcal{B}_j),$$

$$\Sigma'_C = \mathbb{E} [\hat{C}_k \otimes \hat{C}_k] = \sum_{l=1}^{n_c} \sigma_{c,l}^2 (\mathcal{C}_l \otimes \mathcal{C}_l).$$

Then, it is straight forward to see that \mathcal{X}_k evolves as follows

$$\mathcal{X}_{k+1} = H\mathcal{X}_k + \underbrace{\begin{bmatrix} I_n \otimes I_n & 0_{n^2 \times 1} \\ 0_{n^2 \times n^2} & 0_{n^2 \times 1} \\ 0_{n^2 \times n^2} & 0_{n^2 \times 1} \\ 0_{n^2 \times n^2} & L \otimes L \end{bmatrix}}_{:=\Phi} \mathcal{V}, \quad (21)$$

where the matrix H in (21) gathers all the resulting coefficients obtained while expanding the entries of the vector \mathcal{X}_k . The algebra resulting in the following expression of H is available in the appendix of [19]. Since the optimal gain matrices K, L achieve mean-square compensation of the system (1) and (2), the covariance of the estimation error will have a steady state value. Since by assumption, $\bar{A} - L\bar{C}$ is Schur stable, we see that $\mathbb{E}[e_k] \rightarrow 0$ as $k \rightarrow \infty$ regardless of the initial state-residual e_0 which in turn results in $\mathbb{E}[r_k] \rightarrow 0$ as $k \rightarrow \infty$. That is, $\mathbb{E}[e_\infty] = 0 \implies \mathbb{E}[r_\infty] = 0$ and subsequently in steady state,

$$\mathcal{X}_\infty = H\mathcal{X}_\infty + \Phi\mathcal{V}. \quad (22)$$

$$\iff \mathcal{X}_\infty = (I_{4n^2} - H)^{-1}\Phi\mathcal{V}, \quad (23)$$

where $(I_{4n^2} - H)^{-1}$ exists by the mean-square stability assumption of the compensator gains (K, L) . This amounts to solving a (generalized) Lyapunov equation. Such an equation can be solved more efficiently by specialized solvers which do not require the inverse to be computed explicitly; for simplicity we present the equation and its solution in this form. Having obtained \mathcal{X}_∞ , the steady state second moments of the state- and output-residuals can be computed as

$$E_\infty = X_\infty - \tilde{X}_\infty - \check{X}_\infty + \hat{X}_\infty, \quad \text{and} \quad (24)$$

$$R_\infty = (\bar{C} \otimes \bar{C})E_\infty + \Sigma'_C X_\infty + \text{vec}(\Sigma_v). \quad (25)$$

Finally, using the matrix reshaping operator $\text{mat}(\cdot)$, we retrieve the required steady state residual covariance as follows

$$\Sigma_{x_\infty} = \text{mat}(E_\infty, n, n), \quad \text{and} \quad (26)$$

$$\Sigma_r = \text{mat}(R_\infty, p, p). \quad (27)$$

IV. ANOMALY DETECTOR DESIGN WITH RESIDUAL FROM MLQG COMPENSATION

We now present how to analyze the residual obtained from the MLQG compensator and elaborate the procedure to construct the corresponding anomaly detector threshold in this section. Note that the covariance of the residual computed through (20) is a function of covariance matrices of both the additive and multiplicative noises. This is in sharp contrast to the case in [20], [7], [8] where the residual covariance was just a function of the additive noise covariance. Further, to account for the changes in the covariance of the residual, we form a quadratic distance measure as

$$q_k = r_k^\top \Sigma_r^{-1} r_k. \quad (28)$$

It is then straightforward to see that

$$\begin{aligned} \mathbb{E}[q_k] &= \mathbb{E}[r_k^\top \Sigma_r^{-1} r_k] \\ &= \text{Tr}(\Sigma_r^{-1} \Sigma_r) + (\bar{C}e_k)^\top \Sigma_r^{-1} (\bar{C}e_k) \\ &= p + e_k^\top \bar{C}^\top \Sigma_r^{-1} \bar{C} e_k. \end{aligned} \quad (29)$$

which implies that if mean-square compensation through the choice of (K, L) is not qualitatively performed, the resulting mean of the distance measure data, $\mathbb{E}[q_k]$ will diverge to infinity when the multiplicative noise variances are significant enough. Then, for a given q_k from (28) and a threshold $\alpha \in \mathbb{R}_{>0}$ corresponding to a desired false alarm rate \mathcal{F} , the anomaly detector can be designed such that alarm time(s) $k^* \in \mathbb{N}$ are produced according to the following rules

$$\begin{cases} q_k \leq \alpha, & \text{no alarm,} \\ q_k > \alpha, & \text{alarm: } k^* = k. \end{cases} \quad (30)$$

If \mathbb{P}_{r_k} was Gaussian, then q_k would follow the chi-squared distribution, meaning that for a given tail probability defined using \mathcal{F} , the chi-squared detector described as in [2] can be used to obtain the required detector threshold. However, in our setting due to the multiplicative noises, \mathbb{P}_{r_k} is *non-Gaussian* and thereby the chi-squared detector is *not* appropriate. We instead utilize a moment-based approach for constructing the threshold. We propose to use the higher-order moment based anomaly detector design proposed in [7] to design the detector threshold in this setting. The residual q_k is collected for a sufficiently long period of time to form the s -moments based ambiguity set $\mathcal{P}_q^s := \{\mathbb{P}_q \mid \mathbb{E}[q_k^s] = M_q^s\}$. The optimal threshold $\alpha_{q,s}^*$ ³ satisfying

$$\sup_{\mathbb{P}_q \in \mathcal{P}_q^s} \mathbb{P}_q [q_k > \alpha_{q,s}^*] \leq \mathcal{F}, \quad (31)$$

³The two subscripts q, s in $\alpha_{q,s}^*$ denote the random variable and the number of moments considered respectively.

can then be obtained by directly invoking Theorem 4 in [7] corresponding to a given desired false alarm rate \mathcal{F} .

V. NUMERICAL RESULTS

We consider an inverted pendulum with a torque-producing actuator whose dynamics have been linearized about the vertical equilibrium. That is, the pendulum of mass m is suspended by a mass-less rod of length l and the angle θ is measured from the downward vertical with positive counter clockwise direction. The corresponding nonlinear differential equation of the pendulum mass is

$$\ddot{\theta} = m_c \sin(\theta) + \tau, \quad (32)$$

where $m_c = -\frac{g}{l}$ denotes the uncertain mass constant. Let us denote the state vector by $x = [x_1 \ x_2] = [\theta \ \dot{\theta}]$ and the torque input by $u = \tau$. Then, the corresponding discrete time dynamics obtained through the forward Euler discretization of the linearized dynamics of (32) around the equilibrium point $\tilde{x} = (\pi, 0)$ with step size Δt is

$$x_{k+1} = \begin{bmatrix} 1 & \Delta t \\ m_c \Delta t & 1 \end{bmatrix} x_k + \begin{bmatrix} 0 \\ \Delta t \end{bmatrix} u_k + w_k. \quad (33)$$

Uncertainty on the mass constant m_c corresponds to uncertainty on the matrix A . We consider an example where the true mass constant is $m_c = 10$, but the nominal model underestimates it as $m_c = 5$. We take a step size $\Delta t = 0.1$. At discrete time instances, the sensor returns a noisy measurement of the angular position of pendulum. Hence the corresponding linearized noisy output model is,

$$y = \theta + v_k = [1 \ 0] x_k + v_k. \quad (34)$$

Both w_k and v_k are sampled from the multivariate Laplacian (which has heavier tails than Gaussian with same mean and covariance) with zero-mean and covariance $\Sigma_w = 2I_n$, $\Sigma_v = 2I_p$ respectively. The state and control penalty matrices are $Q = I_n$, $R = I_m$ respectively. The multiplicative noise was considered to exist both in the A and C matrices, with the direction matrices being $\mathcal{A}_1 = \begin{bmatrix} 0 & 0 \\ 1 & 0 \end{bmatrix}$ and $\mathcal{C}_1 = [0.1 \ 0]$ with the multiplicative noise variances $\gamma_{k,1} \sim \mathcal{N}(0, \sigma_{a,1}^2)$, $\kappa_{k,1} \sim \mathcal{N}(0, \sigma_{c,1}^2)$ respectively. The non-Gaussian additive primitive noises w_k, v_k along with these multiplicative noises render the traditional chi-squared detector to be ineffective as the system states will evolve to be *non-Gaussian* for all $t > 0$. Through simulation, we collected the quadratic distance measure q_k data for $T = 10^7$ time steps for the above system with multiplicative noises under two different settings namely, 1) using the standard LQG, and 2) using multiplicative noise-driven LQG compensators. The q_k data computed using the MLQG compensator was then used to tune the anomaly detector for a desired false alarm rate of $\mathcal{F} = 5\%$ using Theorem 4 in [7] with $s = 4$ moments in (31) and along with a bisection tolerance of $\epsilon = 10^{-4}$. The resulting moment bound problem was solved using the SOSToolbox on MATLAB with the SeDuMi solver. The code is made publicly available at <https://github.com/TSummersLab/AnomalyDetectionMultiplicativeNoise>

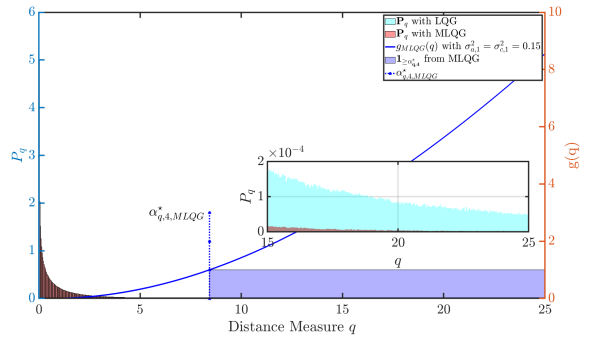


Fig. 2: **Detector Threshold With Multiplicative Noise:** The histograms of the q_k using the LQG and MLQG estimators are shown in cyan and red colors respectively. The moment based polynomial $g(q)$ shown in blue curve bounds the indicator function in shaded blue. The zoomed in histograms clearly indicate the heaviness of the tails (large false alarms) of q_k data in cyan from the LQG compared to the one in red from MLQG even at a low noise multiplicative noise setting.

A. LQG & MLQG with Low Multiplicative Noises

When the system was simulated with low multiplicative noise variances $\sigma_{a,1}^2 = \sigma_{c,1}^2 < 0.10$, the resulting (K, L) matrix pair from both the LQG and the MLQG compensators had similar values and the anomaly detectors from both compensators had similar good performances. However, the performance of MLQG started getting better with $\sigma_{a,1}^2 = \sigma_{c,1}^2 = 0.15$ and the results are shown in Figure 2. The histograms of the q_k data using the LQG and MLQG estimators are shown in cyan and red colors respectively. The q_k data from the MLQG compensator resulted in mean-square compensatability (verified via the convergence of the coupled Riccati equations) and subsequently the corresponding collected q_k data resulted in an optimal detector threshold $\alpha_{q,4}^* = 8.43$ with false alarm rate being 0.87%. On the other hand, when the q_k data collected from the standard LQG was evaluated against the same threshold $\alpha_{q,4}^*$, it resulted in 8.71% false alarms which is clearly greater than the desired false alarm rate of $\mathcal{F} = 5\%$. It is evident from the zoomed-in part of the Figure 2 that the histogram of the q_k data from LQG started depicting heavier tails than the histogram for the MLQG case due to the multiplicative noise and this resulted in increased false alarm rate. Subsequently, we show how LQG's performance deteriorates quickly with even greater multiplicative noise covariance in the next subsection.

B. Effect of Multiplicative Noise Variance on the Worst Case False Alarm Rate

Here, we show how the variances $\sigma_{a,1}^2, \sigma_{c,1}^2$ of the multiplicative noises $\gamma_{k,1}, \kappa_{k,1}$ respectively affect the resulting anomaly detector's worst case false alarm rate. Starting from $\sigma_{a,1}^2 = \sigma_{c,1}^2 = 0.15$, we simulated the system by increasing the variances and the results are in Table I. It is evident that standard LQG results in $\hat{\mathbb{E}}[q_k] \rightarrow \infty$ when the variances were increased starting from 0.15 and subsequently the restriction

var	Σ_r		$\hat{\mathbb{E}}[q_k]$		$\mathcal{F}_{worse}(\%)$		$\alpha_{q,4}^*$
	LQG	MLQG	LQG	MLQG	LQG	MLQG	
0.15	3.65	6.47	25.744	1.011	8.71	0.87	8.43
0.30	4.99	6.95	3.3×10^{11}	1.019	28.48	0.82	8.75
0.45	5.14	7.40	2.6×10^{53}	1.026	74.52	0.71	9.33
\vdots	\vdots	\vdots	∞	\vdots	\vdots	\vdots	\vdots
3.80	5.31	N/A	∞	N/A	N/A	N/A	N/A

TABLE I: Effect of varying the multiplicative noise variances ($\sigma_{a,1}^2 = \sigma_{c,1}^2 = \text{var}$) on the resulting steady state Σ_r , optimal threshold $\alpha_{q,4}^*$, sample based mean $\hat{\mathbb{E}}[q_k]$ and the worst case false alarm rates \mathcal{F}_{worse} from the standard LQG & the MLQG compensators are shown here. It is evident that the MLQG mean-square compensate the system better than the standard LQG with increasing multiplicative noise variances.

of not being able to use even the Markov bound in this case made us to evaluate the q_k data against the threshold obtained using MLQG approach instead. On the other hand, MLQG compensator was capable of mean-square compensate the system with increasing covariances by resulting in finite mean (approximately equal to 1 and thereby agreeing with (29)). Starting from $\sigma_{a,1}^2 = \sigma_{c,1}^2 \geq 0.50$, numerical issues started accompanying the threshold calculations due to exploding values of the moments (can be addressed using orthogonal basis such as the Legendre polynomial basis to provide numerical stability). Specifically, when the variances were increased beyond $\sigma_{a,1}^2 = \sigma_{c,1}^2 \geq 3.8$, MLQG stopped converging as mean-square compensation was lost for such higher variance multiplicative noises. The effect of increasing variance also affected the resulting false alarm rates when the residuals from the standard LQG and the MLQG compensators were compared against the threshold computed using from the MLQG residuals. The resulting optimal threshold $\alpha_{q,4}^*$ increased when the multiplicative noise variances increased. For this reason, in this problem setting the false alarm rate of MLQG happened to decrease with increased multiplicative noise variance; there is a nontrivial relation between the multiplicative noise variances and the threshold designed by the detection scheme, which depends e.g. on the coupled Riccati equation solution. As shown in Table I, the MLQG with finite set of $s = 4$ empirical moments starting from $\hat{\mathbb{E}}[q_k]$ guaranteed that the resulting worst case false alarm rate are always upper bounded by the desired value of $\mathcal{F} = 5\%$. On the other hand, the standard LQG resulted in worst case false alarms that were monotonically becoming significantly greater than the desired value of $\mathcal{F} = 5\%$.

VI. CONCLUSION

An extension of the state-of-the-art anomaly detection algorithms for CPS with modeling errors via the multiplicative noise framework was discussed in this paper. The multiplicative noise-driven LQG being a robust state estimator was used to hedge against the model risk to construct the state estimate. The proposed method was demonstrated using a numerical simulation. Future work seeks to investigate the setting where the multiplicative noise distributions are

unknown and to obtain online estimates of the system dynamics through system identification technique combined with the above compensator for implementing data-driven distributionally robust anomaly detection for vulnerable CPS.

REFERENCES

- [1] J. Giraldo, D. Urbina, A. Cardenas, J. Valente, M. Faisal, J. Ruths, N. O. Tippenhauer, H. Sandberg, and R. Candell, “A survey of physics-based attack detection in cyber-physical systems,” *ACM Comput. Surv.*, vol. 51, no. 4, Jul. 2018.
- [2] N. Hashemi and J. Ruths, “Generalized chi-squared detector for LTI systems with non-gaussian noise,” in *2019 American Control Conference (ACC)*, 2019, pp. 404–410.
- [3] F. Pasqualetti, F. Dorfler, and F. Bullo, “Attack detection and identification in cyber-physical systems,” *IEEE Transactions on Automatic Control*, vol. 58, pp. 2715–2729, 2013.
- [4] J. Goh and M. Sim, “Distributionally robust optimization and its tractable approximations,” *Operations research*, vol. 58, no. 4-part-1, pp. 902–917, 2010.
- [5] P. M. Esfahani and D. Kuhn, “Data-driven distributionally robust optimization using the wasserstein metric: Performance guarantees and tractable reformulations,” *Mathematical Programming*, vol. 171, no. 1-2, pp. 115–166, 2018.
- [6] W. Wiesemann, D. Kuhn, and M. Sim, “Distributionally robust convex optimization,” *Operations Research*, vol. 62, no. 6, pp. 1358–1376, 2014.
- [7] V. Renganathan, N. Hashemi, J. Ruths, and T. H. Summers, “Higher-order moment-based anomaly detection,” *IEEE Control Systems Letters*, vol. 6, pp. 211–216, 2022.
- [8] ———, “Distributionally robust tuning of anomaly detectors in cyber-physical systems with stealthy attacks,” in *2020 American Control Conference (ACC)*. IEEE, 2020, pp. 1247–1252.
- [9] D. Li and S. Martinez, “High-confidence attack detection via wasserstein-metric computations,” *IEEE Control Systems Letters*, vol. 5, no. 2, pp. 379–384, 2020.
- [10] W. Li, E. Todorov, and R. E. Skelton, “Estimation and control of systems with multiplicative noise via linear matrix inequalities,” in *Proceedings of the 2005 American Control Conference, 2005*. IEEE, 2005, pp. 1811–1816.
- [11] B. J. Gravell, P. M. Esfahani, and T. H. Summers, “Robust control design for linear systems via multiplicative noise,” *IFAC-PapersOnLine*, vol. 53, no. 2, pp. 7392–7399, 2020.
- [12] B. Gravell, P. Mohajerin Esfahani, and T. Summers, “Learning optimal controllers for linear systems with multiplicative noise via policy gradient,” *IEEE Transactions on Automatic Control*, 2021.
- [13] B. C. Levy and R. Nikoukhah, “Robust state space filtering under incremental model perturbations subject to a relative entropy tolerance,” *IEEE Transactions on Automatic Control*, vol. 58, no. 3, pp. 682–695, 2012.
- [14] M. Zorzi, “Robust kalman filtering under model perturbations,” *IEEE Transactions on Automatic Control*, vol. 62, no. 6, pp. 2902–2907, 2017.
- [15] S. Shafeezadeh Abadeh, V. A. Nguyen, D. Kuhn, and P. M. Mohajerin Esfahani, “Wasserstein distributionally robust kalman filtering,” in *Advances in Neural Information Processing Systems*, vol. 31. Curran Associates, Inc., 2018.
- [16] R. E. Kalman *et al.*, “Contributions to the theory of optimal control,” *Bol. soc. mat. mexicana*, vol. 5, no. 2, pp. 102–119, 1960.
- [17] W. L. De Koning, “Compensatability and optimal compensation of systems with white parameters,” *IEEE Transactions on Automatic Control*, vol. 37, no. 5, pp. 579–588, 1992.
- [18] L. El Ghaoui, “State-feedback control of systems with multiplicative noise via linear matrix inequalities,” *Systems & Control Letters*, vol. 24, no. 3, pp. 223–228, 1995.
- [19] V. Renganathan, B. J. Gravell, J. Ruths, and T. H. Summers, “Anomaly detection under multiplicative noise model uncertainty,” *arXiv preprint arXiv:2103.15228*, 2021.
- [20] N. Hashemi, C. Murguia, and J. Ruths, “A comparison of stealthy sensor attacks on control systems,” in *2018 Annual American Control Conference (ACC)*, 2018, pp. 973–979.

APPENDIX I MOMENT DYNAMICS

Recall the closed-loop system equations:

$$\begin{aligned} x_{k+1} &= A_k x_k + B_k u_k + w_k, \\ \hat{x}_{k+1} &= \bar{A} \hat{x}_k + \bar{B} u_k + L(y_k - \hat{y}_k), \\ u_k &= K \hat{x}_k, \\ y_k &= C_k x_k + v_k, \\ \hat{y}_k &= \bar{C} \hat{x}_k, \end{aligned}$$

and the state- and output-residuals

$$\begin{aligned} e_k &= x_k - \hat{x}_k, \\ r_k &= y_k - \hat{y}_k. \end{aligned}$$

Denote

$$\begin{aligned} \Sigma'_A &= \mathbb{E} \left[\hat{A}_k \otimes \hat{A}_k \right] = \sum_{i=1}^{n_a} \sigma_{a,i}^2 (\mathcal{A}_i \otimes \mathcal{A}_i), \\ \Sigma'_B &= \mathbb{E} \left[\hat{B}_k \otimes \hat{B}_k \right] = \sum_{j=1}^{n_b} \sigma_{b,j}^2 (\mathcal{B}_j \otimes \mathcal{B}_j), \\ \Sigma'_C &= \mathbb{E} \left[\hat{C}_k \otimes \hat{C}_k \right] = \sum_{l=1}^{n_c} \sigma_{c,l}^2 (\mathcal{C}_l \otimes \mathcal{C}_l). \end{aligned}$$

Hence, we have the identities

$$\begin{aligned} \mathbb{E}[A_k \otimes A_k] &= \bar{A} \otimes \bar{A} + \Sigma'_A, \\ \mathbb{E}[B_k \otimes B_k] &= \bar{B} \otimes \bar{B} + \Sigma'_B, \\ \mathbb{E}[C_k \otimes C_k] &= \bar{C} \otimes \bar{C} + \Sigma'_C. \end{aligned}$$

While studying the moment dynamics, we shall readily employ the zero-mean and zero-correlation assumptions of \hat{A}_k , \hat{B}_k , \hat{C}_k , w_k , and v_k in the following derivations.

A. First moment dynamics

The expected output-residual is

$$\mathbb{E}[r_k] = \mathbb{E}[y_k - \hat{y}_k] = \mathbb{E}[C_k x_k + v_k - \bar{C} \hat{x}_k] = \mathbb{E}[C_k x_k] - \bar{C} \mathbb{E}[\hat{x}_k] = \bar{C} e_k. \quad (35)$$

The expected state-residual evolves as

$$\begin{aligned} \mathbb{E}[e_{k+1}] &= \mathbb{E}[x_{k+1} - \hat{x}_{k+1}] \\ &= \mathbb{E}[x_{k+1}] - \mathbb{E}[\hat{x}_{k+1}] \\ &= \mathbb{E}[A_k x_k + B_k K \hat{x}_k + w_k] - \mathbb{E}[\bar{A} \hat{x}_k + \bar{B} K \hat{x}_k + L(y_k - \hat{y}_k)] \quad (36) \\ &= \bar{A} \mathbb{E}[x_k] + \bar{B} K \mathbb{E}[\hat{x}_k] - (\bar{A} + \bar{B} K) \mathbb{E}[\hat{x}_k] - L \mathbb{E}[y_k - \hat{y}_k] \\ &= \bar{A} \mathbb{E}[x_k] + \bar{B} K \mathbb{E}[\hat{x}_k] - (\bar{A} + \bar{B} K) \mathbb{E}[\hat{x}_k] - L \bar{C} e_k \\ &= \bar{A} \mathbb{E}[x_k] - \bar{A} \mathbb{E}[\hat{x}_k] + \bar{B} K \mathbb{E}[\hat{x}_k] - \bar{B} K \mathbb{E}[\hat{x}_k] - L \bar{C} e_k \\ &= (\bar{A} - L \bar{C}) e_k. \quad (37) \end{aligned}$$

B. Second moment dynamics

For the state and state-estimate second moment dynamics, denote

$$\begin{aligned} X_k &= \text{vec} \mathbb{E} [x_k x_k^\top], \quad \tilde{X}_k = \text{vec} \mathbb{E} [x_k \hat{x}_k^\top], \\ \tilde{X}_k &= \text{vec} \mathbb{E} [\hat{x}_k x_k^\top], \quad \hat{X}_k = \text{vec} \mathbb{E} [\hat{x}_k \hat{x}_k^\top]. \end{aligned}$$

We have

$$\begin{aligned}
X_{k+1} &= \text{vec} \mathbb{E} [x_{k+1} x_{k+1}^\top] \\
&= \text{vec} \mathbb{E} [(A_k x_k + B_k K \hat{x}_k + w_k)(A_k x_k + B_k K \hat{x}_k + w_k)^\top] \\
&= (\bar{A} \otimes \bar{A} + \Sigma'_A) X_k + ((\bar{B}K) \otimes \bar{A}) \tilde{X}_k + (\bar{A} \otimes (\bar{B}K)) \check{X}_k + (\bar{B} \otimes \bar{B} + \Sigma'_B) (K \otimes K) \hat{X}_k + \text{vec}(\Sigma_w),
\end{aligned} \tag{38}$$

and

$$\begin{aligned}
\tilde{X}_{k+1} &= \text{vec} \mathbb{E} [x_{k+1} \hat{x}_{k+1}^\top] \\
&= \text{vec} \mathbb{E} [(A_k x_k + B_k K \hat{x}_k + w_k) (LC_k x_k + (\bar{A} + \bar{B}K - L\bar{C}) \hat{x}_k + Lv_k)^\top] \\
&= ((L\bar{C}) \otimes \bar{A}) X_k + ((\bar{A} + \bar{B}K - L\bar{C}) \otimes \bar{A}) \tilde{X}_k + ((L\bar{C}) \otimes (\bar{B}K)) \check{X}_k + ((\bar{A} + \bar{B}K - L\bar{C}) \otimes (\bar{B}K)) \hat{X}_k,
\end{aligned} \tag{39}$$

and

$$\begin{aligned}
\check{X}_{k+1} &= \text{vec} \mathbb{E} [\hat{x}_{k+1} x_{k+1}^\top] \\
&= \text{vec} \mathbb{E} [(LC_k x_k + (\bar{A} + \bar{B}K - L\bar{C}) \hat{x}_k + Lv_k) (A_k x_k + B_k K \hat{x}_k + w_k)^\top] \\
&= (\bar{A} \otimes (L\bar{C})) X_k + ((\bar{B}K) \otimes (L\bar{C})) \tilde{X}_k + (\bar{A} \otimes (\bar{A} + \bar{B}K - L\bar{C})) \check{X}_k + ((\bar{B}K) \otimes (\bar{A} + \bar{B}K - L\bar{C})) \hat{X}_k,
\end{aligned} \tag{40}$$

and

$$\begin{aligned}
\hat{X}_{k+1} &= \text{vec} \mathbb{E} [\hat{x}_{k+1} \hat{x}_{k+1}^\top] \\
&= \text{vec} \mathbb{E} [(LC_k x_k + (\bar{A} + \bar{B}K - L\bar{C}) \hat{x}_k + Lv_k) (LC_k x_k + (\bar{A} + \bar{B}K - L\bar{C}) \hat{x}_k + Lv_k)^\top] \\
&= (L \otimes L)(\bar{C} \otimes \bar{C} + \Sigma'_C) X_k + ((\bar{A} + \bar{B}K - L\bar{C}) \otimes (L\bar{C})) \tilde{X}_k \\
&\quad + ((L\bar{C}) \otimes (\bar{A} + \bar{B}K - L\bar{C})) \check{X}_k + ((\bar{A} + \bar{B}K - L\bar{C}) \otimes (\bar{A} + \bar{B}K - L\bar{C})) \hat{X}_k + (L \otimes L) \text{vec}(\Sigma_v).
\end{aligned} \tag{41}$$

Define

$$\mathcal{X}_k := \begin{bmatrix} X_k \\ \tilde{X}_k \\ \check{X}_k \\ \hat{X}_k \end{bmatrix}, \quad \text{and} \quad \mathcal{V} := \begin{bmatrix} \text{vec}(\Sigma_w) \\ \text{vec}(\Sigma_v) \end{bmatrix}.$$

By gathering the matrix coefficients in equations (38), (39), (40), (41) as

$$H := \begin{bmatrix} \bar{A} \otimes \bar{A} + \Sigma'_A & (\bar{B}K) \otimes \bar{A} & \bar{A} \otimes (\bar{B}K) & (\bar{B} \otimes \bar{B} + \Sigma'_B) (K \otimes K) \\ (\bar{L}\bar{C}) \otimes \bar{A} & (\bar{A} + \bar{B}K - L\bar{C}) \otimes \bar{A} & (\bar{L}\bar{C}) \otimes (\bar{B}K) & (\bar{A} + \bar{B}K - L\bar{C}) \otimes (\bar{B}K) \\ \bar{A} \otimes (L\bar{C}) & (\bar{B}K) \otimes (L\bar{C}) & \bar{A} \otimes (\bar{A} + \bar{B}K - L\bar{C}) & (\bar{B}K) \otimes (\bar{A} + \bar{B}K - L\bar{C}) \\ (L \otimes L)(\bar{C} \otimes \bar{C} + \Sigma'_C) & (\bar{A} + \bar{B}K - L\bar{C}) \otimes (L\bar{C}) & (L\bar{C}) \otimes (\bar{A} + \bar{B}K - L\bar{C}) & (\bar{A} + \bar{B}K - L\bar{C}) \otimes (\bar{A} + \bar{B}K - L\bar{C}) \end{bmatrix}$$

and

$$\Phi := \begin{bmatrix} I_n \otimes I_n & 0_{n^2 \times 1} \\ 0_{n^2 \times n^2} & 0_{n^2 \times 1} \\ 0_{n^2 \times n^2} & 0_{n^2 \times 1} \\ 0_{n^2 \times n^2} & L \otimes L \end{bmatrix}$$

we have the compact representation of (38), (39), (40), (41) as

$$\mathcal{X}_{k+1} = H \mathcal{X}_k + \Phi \mathcal{V} \tag{42}$$

For the state- and output-residual second moments, denote $E_k = \text{vec} \mathbb{E} [e_k e_k^\top]$ $R_k = \text{vec} \mathbb{E} [r_k r_k^\top]$. We have

$$\begin{aligned}
E_k &= \text{vec} \mathbb{E} [e_k e_k^\top] \\
&= \text{vec} \mathbb{E} [(x_k - \hat{x}_k)(x_k - \hat{x}_k)^\top] \\
&= X_k - \tilde{X}_k - \check{X}_k + \hat{X}_k
\end{aligned} \tag{43}$$

and

$$\begin{aligned}
R_k &= \text{vec} \mathbb{E} [r_k r_k^\top] \\
&= \text{vec} \mathbb{E} [(y_k - \hat{y}_k)(y_k - \hat{y}_k)^\top] \\
&= \text{vec} \mathbb{E} [(C_k x_k + v_k - \bar{C} \hat{x}_k)(C_k x_k + v_k - \bar{C} \hat{x}_k)^\top] \\
&= \text{vec} \mathbb{E} [(\bar{C}(x_k - \hat{x}_k) + (C_k - \bar{C})x_k + v_k)(\bar{C}(x_k - \hat{x}_k) + (C_k - \bar{C})x_k + v_k)^\top] \\
&= (\bar{C} \otimes \bar{C}) E_k + \Sigma'_C X_k + \text{vec}(\Sigma_v)
\end{aligned} \tag{44}$$